

## Atomic coordination and the distribution of electric field gradients in amorphous solids

G. Czjzek, J. Fink, F. Götz, and H. Schmidt

*Kernforschungszentrum Karlsruhe GmbH, Institut für Angewandte Kernphysik, Postfach 3640, D-7500 Karlsruhe, Federal Republic of Germany*

J. M. D. Coey\* and J.-P. Rebouillat

*Groupe des Transitions de Phases<sup>1</sup> and Laboratoire Louis Néel,<sup>1</sup> Centre Nationale de la Recherche Scientifique, B.P. 166, F-38042 Grenoble Cédex, France*

A. Liénard

*Commissariat à l'Energie Atomique, L.E.T.I., N.C.E., B.P. 85, F-38041 Grenoble Cédex, France*

(Received 25 July 1980)

The observation of nuclear quadrupole interactions in amorphous solids provides a unique possibility of obtaining information about the angular distribution of local ionic coordinations, complementary to the information about radial distributions deduced from x-ray and neutron diffraction and from extended x-ray absorption fine structure measurements. In the present paper the relation between ionic coordinations and the distribution of electric field gradients (EFG) is investigated. It is shown that the distribution function  $P(V_{zz}, \eta)$  of the splitting parameters  $V_{zz}$  (the electric field gradient) and  $\eta$  (the asymmetry parameter) in general yields zero probability both for  $V_{zz} = 0$  and for  $\eta = 0$ . For solids which are isotropic on the average, the distribution function of the components  $V_{ik}$  of the EFG tensor depends only on two variables, the invariant functions of the tensor components [ $\text{Det}(V_{ik})$  and  $\Sigma V_{ik}^2$ ]. Expressions for these quantities in terms of the radial coordinates of the ions causing the EFG and of the bond angles between pairs of ions are given. For amorphous solids with random ionic coordination an analytic approximation for the distribution function  $P(V_{zz}, \eta)$  is derived. This function is strongly dominated by the distribution of ions in the first coordination shell. The results are applied to the analysis of Mössbauer spectra of  $^{155}\text{Gd}$  in amorphous Gd-Ni alloys.

### I. INTRODUCTION

Our knowledge of atomic coordination in amorphous solids is rather limited although many experimental investigations of the atomic structure of amorphous materials have been performed. A basic limitation is inherent in the prevailing source of experimental information: x-ray and neutron diffraction, since diffraction patterns are primarily determined by *radial* pair-distribution functions. Inferences on the *directional* characteristics of short-range atomic coordination can be obtained only indirectly, via comparison with specific models, and in general they lack conclusive power. The alternative method applied in structural investigations of amorphous solids, EXAFS (extended x-ray absorption fine structure), is more sensitive to details of the local atomic coordination, but again the experimental results are determined by the number and radial distances of atoms in the first few coordination shells and carry no information on their angular distribution.

Thus, experimental results obtained by these methods are not well suited for distinguishing between structural models for amorphous metals and alloys based either on dense random packing of hard spheres<sup>1</sup> (DRPHS) or on models stressing

the preservation of chemical bonding requirements, specifically of bond angles, in local atomic coordinations.<sup>2</sup>

In this situation the exploitation of experimental techniques capable of yielding supplementary information on angular atomic coordinations is highly desirable. One possibility is provided by the interaction between the quadrupole moment of atomic nuclei and the electric field gradient (EFG) originating from the distribution of electric charges around the nuclei, the electric quadrupole interaction. This interaction can be observed experimentally by nuclear magnetic resonance,<sup>3</sup> by Mössbauer spectroscopy,<sup>4</sup> or by measurements of perturbed angular correlations.<sup>5</sup>

Although many experimental observations of quadrupole interactions in amorphous solids have been reported,<sup>6-12</sup> mostly by NMR or Mössbauer spectroscopy, the results have been analyzed with respect to their significance for structural information only to a limited extent.<sup>7-10</sup>

Several studies have been devoted to the closely related problem of the distribution of crystal-field splittings in amorphous alloys.<sup>13,14</sup> Apart from different shielding factors, the EFG caused by charges outside the own electronic shell of the probe nucleus is identical to the crystal field of second order acting on the electrons located at

this nucleus. According to the random anisotropy model,<sup>15</sup> which is quite successful in describing the magnetic properties of amorphous alloys containing rare-earth ions, the crystal field of second order along with exchange interactions plays a dominant role in determining these magnetic properties. In this context Cochrane *et al.*<sup>13</sup> have investigated the distribution of level splittings of an electronic state with total angular momentum  $J=1$  due to the charge distribution derived from a DRPHS model. Their results are quite similar to those obtained in analogous calculations for the nuclear quadrupole interaction,<sup>7,8</sup> as may be expected in view of the above-mentioned equivalence between the two problems. The possibility of obtaining direct experimental information on the crystal-field distribution in amorphous solids via measurements of the quadrupole interaction is another source of interest for investigations of this kind.

In all cases referred to the experimental data were compared with distributions of energy levels or splitting parameters derived from computer simulations of the amorphous structure in the framework of DRPHS models. A general investigation of the relation between ionic coordination and level distribution has not yet been attempted. The present paper is devoted to this subject. In Sec. II we expound the basic definitions and relations needed. Then we demonstrate that the task is simplified if we assume the material under study to be isotropic on the average. The assumption of overall isotropy is appropriate in principle<sup>16</sup> for several types of amorphous solids: amorphous metals and alloys, tetrahedrally coordinated semiconductors, and for most oxide glasses. In Sec. III we concentrate on amorphous solids with randomly arranged ions, deriving an analytic approximation for the distribution function of the splitting parameters for this case. The results obtained in Sec. III are then applied to the analysis of <sup>155</sup>Gd Mössbauer spectra of amorphous Gd-Ni alloys in Sec. IV.

In our calculations we make use of two essential approximations:

(i) In our considerations of random amorphous structures we treat the ions as hard spheres. This approach has generally yielded good approximations for statistical aspects of amorphous metallic solids and simple liquids such as radial pair-distribution functions and particularly in the evaluation of excluded volume effects.<sup>17</sup> Since these aspects are of primary importance in the present work, we may expect the hard-sphere approach to yield reasonable results.

(ii) Calculations of the EFG are carried out in a point-charge model. This approach often yields

wrong values for the EFG, especially in metallic solids where the conduction electrons strongly contribute to the EFG.<sup>18</sup> The empirical correlation between experimental EFG values and those calculated in the point charge model which has been established for a large number of metallic solids,<sup>19</sup> however, shows that the response of the conduction electrons to the potential due to the skeleton of ionic charges leads to a contribution which is approximately proportional to the EFG generated by the ionic charges. Insofar as this proportionality holds, the essential result derived in the present work, the functional form of the distribution functions, is not affected. Only the numerical values of the parameters appearing in the distribution functions will be different from the results obtained by point charge calculations.

We have completely disregarded contributions of the local valence electrons to the EFG. In practical applications the possible existence of such contributions has to be considered carefully as they may dominate the observed quadrupole splitting, particularly in the case of rare-earth ions.

In our work we have profited from the fact that our problem is a special case of the broader subject of random matrices which has been investigated thoroughly in connection with the statistical theory of nuclear energy levels.<sup>20</sup> There the interest has focused on  $N \times N$  matrices with large  $N$ , whereas we have to deal with  $3 \times 3$  matrices with the additional restriction of zero trace. Nevertheless some of the general results can be applied in our case.

## II. RELATION BETWEEN IONIC COORDINATION AND EFG DISTRIBUTION

### A. The EFG tensor

The term in the hyperfine Hamiltonian due to the nuclear quadrupole interaction (Refs. 3, 4, and 21),  $H_Q = \bar{Q} : \bar{V}$ , is the product of two tensor quantities: the nuclear quadrupole moment tensor  $\bar{Q}$  which is a measure for the deviation of the nuclear charge distribution from spherical shape and the EFG tensor  $\bar{V}$ .

The components  $V_{ik}$  of the EFG tensor caused by an assembly of discrete charges  $q_n$  (with Cartesian coordinates  $x_i^{(n)}$ , polar coordinates  $r_n, \theta_n, \phi_n$ ) at a nucleus (whose position defines the origin of the coordinate system) are defined by

$$V_{ik} = \sum_n q_n (3x_i^{(n)}x_k^{(n)} - r_n^2\delta_{ik})r_n^{-5}. \quad (1)$$

This  $3 \times 3$  tensor is symmetric ( $V_{ki} = V_{ik}$ ) and has zero trace ( $\sum_i V_{ii} = 0$ ). Thus, it is determined by five independent quantities which can be expressed

in terms of the spherical harmonics  $Y_2^m(\theta_n, \phi_n)$  ( $m=0, \pm 1, \pm 2$ ) of order 2:

$$V_2^m = \sum_n q_n Y_2^m(\theta_n, \phi_n) r_n^{-3}. \quad (2)$$

The quantities  $V_2^m$  are complex, and the calculations are carried through more conveniently in terms of real equivalents  $U_m$ :

$$\begin{aligned} U_0 &= V_2^0 = \frac{1}{2} \sum_n q_n (3 \cos^2 \theta_n - 1) r_n^{-3}, \\ U_1 &= \frac{1}{\sqrt{2}} (V_2^1 + V_2^{-1}) = \sqrt{3} \sum_n q_n \sin \theta_n \cos \theta_n \cos \phi_n r_n^{-3}, \\ U_2 &= \frac{1}{i\sqrt{2}} (V_2^1 - V_2^{-1}) = \sqrt{3} \sum_n q_n \sin \theta_n \cos \theta_n \sin \phi_n r_n^{-3}, \\ U_3 &= \frac{1}{i\sqrt{2}} (V_2^2 - V_2^{-2}) = \frac{1}{2} \sqrt{3} \sum_n q_n \sin^2 \theta_n \sin^2 \phi_n r_n^{-3}, \\ U_4 &= \frac{1}{\sqrt{2}} (V_2^2 + V_2^{-2}) = \frac{1}{2} \sqrt{3} \sum_n q_n \sin^2 \theta_n \cos^2 \phi_n r_n^{-3}. \end{aligned} \quad (3)$$

The tensor components  $V_{ik}$  are linear combinations of the quantities  $U_m$ .

By a suitable choice of the coordinate system, that is, by some rotation defined by the Euler angles  $(\alpha, \beta, \gamma)$ , the tensor  $\vec{V}$  can be diagonalized. Formally, this operation is expressed in terms of a unitary matrix  $\vec{R}(\alpha, \beta, \gamma)$ :

$$\vec{V}^D = \vec{R}(\alpha, \beta, \gamma) \vec{V} \vec{R}^{-1}(\alpha, \beta, \gamma). \quad (4)$$

The splitting of nuclear energy levels depends only on two parameters related to the components of the diagonalized tensor  $\vec{V}^D$ , not on the Euler angles  $(\alpha, \beta, \gamma)$ . The splitting parameters are usually chosen<sup>4</sup> as  $V_{zz}^D$  and the asymmetry parameter  $\eta = (V_{xx}^D - V_{yy}^D)/V_{zz}^D$  with the convention  $|V_{xx}^D| \leq |V_{yy}^D| \leq |V_{zz}^D|$  so that  $0 \leq \eta \leq 1$ . In the following we will omit the superscript  $D$  and write  $V_{zz}$  for  $V_{zz}^D$  as no ambiguity can arise. The spectrum of energy levels of nuclei in amorphous solids is described by the distribution  $P(V_{zz}, \eta)$  of the splitting parameters.

#### B. The distribution function $P(V_{zz}, \eta)$ : General results

The basic distribution determining the physical quantities of interest is the spatial distribution of the ionic charges  $q_n$ . Any structural model of an amorphous solid entails a distribution function of the charges  $q_n$  and of their coordinates  $(r_n, \theta_n, \phi_n)$ .

Our task is then to establish the connection between the structural model and the distribution function  $P(V_{zz}, \eta)$ . This can be divided into two steps.

(i) Derivation of the distribution function  $P_u(U_0, U_1, U_2, U_3, U_4)$  [abbreviated notation:  $P_u(\dots U_m \dots)$ ] of the quantities  $U_m$  from the distribution of the structural parameters  $(q_n; r_n, \theta_n, \phi_n)$  using Eqs. (3). We see no possibility of expressing the relation between  $P_u(\dots U_m \dots)$  and the distribution of the structural parameters in general terms. The following sections will deal with this relation for specific structural models.

(ii) From the distribution function  $P_u(\dots U_m \dots)$  obtained in step (i) the function  $P(V_{zz}, \eta)$  must be derived. The inverse of Eq. (4) expresses the quantities  $U_m$  as functions of  $V_{zz}, \eta$ , and of the Euler angles  $(\alpha, \beta, \gamma)$  when the explicit form<sup>22</sup> of the transformation matrix  $R(\alpha, \beta, \gamma)$  is substituted.

Adapting a formula derived by Porter and Rosenzweig<sup>23</sup> in establishing the relation between the distribution function of the eigenvalues of a real symmetric matrix and the distribution function of the matrix elements we obtain for the functional determinant the expression

$$\left| \frac{\partial(U_0, U_1, U_2, U_3, U_4)}{\partial(V_{zz}, \eta; \alpha, \beta, \gamma)} \right| = 2 \sin \beta V_{zz}^4 \eta (1 - \eta^2/9). \quad (5)$$

Thus, the general solution for the second part of the problem is

$$\begin{aligned} P(V_{zz}, \eta) &= 2 V_{zz}^4 \eta (1 - \eta^2/9) \\ &\times \int d\alpha \int d\beta \int d\gamma \sin \beta P_u(\dots U_m \dots). \end{aligned} \quad (6)$$

This result shows general features worth noticing.

(a) The distribution of  $V_{zz}$  in general exhibits a "hole" around  $V_{zz} = 0$  with zero probability for  $V_{zz} = 0$  and very small probabilities for small values of  $V_{zz}$  unless the distribution function  $P_u(\dots U_m \dots)$  has a strong singularity for  $V_{zz} = 0$ . The physical significance of this result is the vanishingly small probability for highly symmetric configurations—unless the structure strongly favors symmetric configurations such that the function  $P_u(\dots U_m \dots)$  diverges like  $V_{zz}^{-4}$  for  $V_{zz} \rightarrow 0$ . The mathematical origin lies in the form of the relationship between the parameters  $U_m$  and the set of parameters  $(V_{zz}, \eta; \alpha, \beta, \gamma)$ :  $V_{zz}$  plays the role of a radial variable in the five-dimensional space of the parameters  $U_m$ . This feature of  $P(V_{zz}, \eta)$  is reminiscent of the hole in the distribution of molecular fields in a spin glass.<sup>24</sup>

(b) Similarly, the case of axial symmetry,  $\eta = 0$ , or equivalently  $V_{xx} = V_{yy}$ , in general has zero probability. The dependence of the function  $P(V_{zz}, \eta)$  upon  $\eta$  may have significant consequences for the magnetic properties<sup>25</sup> as well as for the

electronic specific heat<sup>26</sup> of amorphous rare-earth alloys.

### C. The isotropic solid

For an amorphous solid which is isotropic on the average, the function  $P_u(\dots U_m \dots)$  must be independent of the choice of coordinates. Consequently,  $P_u(\dots U_m \dots)$  depends exclusively upon invariant functions of the tensor components  $V_{ik}$ . For symmetric  $3 \times 3$  tensors in general there exist three independent invariants<sup>27</sup>: the trace, the sum of squares of the tensor components, and the determinant. Since for the EFG tensor the trace is zero, the arguments of the distribution function are the remaining two invariants. We define

$$S = \frac{2}{3} \sum_{i=1}^3 \sum_{k=1}^3 V_{ik}^2 = \sum_{m=0}^4 U_m^2 = V_{zz}^2 (1 + \eta^2/3) \quad (7)$$

and

$$\begin{aligned} D &= 4 \text{Det}(V) \\ &= U_0^3 + \frac{3}{2} U_0 (U_1^2 + U_2^2 - 2U_3^2 - 2U_4^2) \\ &\quad + \frac{3}{2} \sqrt{3} U_4 (U_1^2 - U_2^2) + 3\sqrt{3} U_1 U_2 U_3, \\ &= V_{zz}^3 (1 - \eta^2). \end{aligned} \quad (8)$$

The expressions for  $S$  and  $D$  in terms of  $V_{zz}$  and  $\eta$  show that these two quantities are not completely independent—a consequence of the vanishing trace:

$$S = \sum_{i < j} \frac{q_i q_j}{r_i^3 r_j^3} (3 \cos^2 \Theta_{ij} - 1) + \sum_i \left( \frac{q_i}{r_i^3} \right)^2, \quad (12)$$

$$\begin{aligned} D &= 3 \sum_{i < j < k} \frac{q_i q_j q_k}{r_i^3 r_j^3 r_k^3} [9 \cos \Theta_{ij} \cos \Theta_{ik} \cos \Theta_{jk} - 3(\cos^2 \Theta_{ij} + \cos^2 \Theta_{ik} + \cos^2 \Theta_{jk}) + 2] \\ &\quad + \frac{3}{2} \sum_{i < j} \frac{q_i q_j}{r_i^3 r_j^3} \left( \frac{q_i}{r_i^3} + \frac{q_j}{r_j^3} \right) (3 \cos^2 \Theta_{ij} - 1) + \sum_i \left( \frac{q_i}{r_i^3} \right)^3. \end{aligned} \quad (13)$$

According to these equations, the function  $G(S) = \int F(D, S) dD$  is related to the angular pair-distribution function  $g(\Theta_{12})$ : If  $g$  is expressed as function of  $\cos^2 \Theta_{12}$ , then  $G(S)$  is obtained from this function by  $N_I(N_I - 1)/2$  folding operations if the total number of ions is  $N_I$ . The dependence of  $F(D, S)$  upon  $D$ , on the other hand, involves triple correlations. Thus, experimental investigations of the EFG distribution in isotropic amorphous solids yield information about these angular correlations.

The reduced dimension of the parameter space in which the distribution function is defined obviously simplifies the task of finding the connection between a structural model and the corresponding EFG distribution. On the other hand, Eqs. (12) and (13) at first sight appear more complicated than the original equations (3) which have

$$0 \leq D^2/S^3 = (1 - \eta^2)^2 / (1 + \eta^2/3)^3 \leq 1. \quad (9)$$

This restriction is accounted for by introducing the step function  $\Theta(S^3 - D^2)$  in the distribution function. Thus, for an isotropic solid we can replace  $P_u(\dots U_m \dots) \Pi_m dU_m$  by  $\Theta(S^3 - D^2) \times F(D, S) dD dS$ .

The transformation of the distribution function to the  $V_{zz}, \eta$  representation is simplified since  $P_u(\dots U_m \dots)$  does not depend upon the Euler angles. Thus, the integrations over  $(\alpha, \beta, \gamma)$  yield a constant factor, and Eq. (6) is replaced by

$$P(V_{zz}, \eta) = 6 V_{zz}^4 \eta (1 - \eta^2/9) F(V_{zz}^3 (1 - \eta^2), V_{zz}^2 (1 + \eta^2/3)). \quad (10)$$

The problem denoted as step (i) in the preceding section is now the derivation of the function  $F(D, S)$  from the distribution of structural parameters. By substitution of Eqs. (3) into Eqs. (7) and (8) the quantities  $D$  and  $S$  can be expressed in terms of the radial coordinates  $r_i$  of the ionic charges and of the bond angles  $\Theta_{ij}$  between pairs of ions which are defined by

$$\cos \Theta_{ij} = \cos \theta_i \cos \theta_j + \sin \theta_i \sin \theta_j \cos(\phi_i - \phi_j) \quad (11)$$

in the following way:

the attractive feature of being additive in the contributions of individual ions. However, these expressions for  $S$  and  $D$  probably are quite useful for calculations of the EFG distribution caused by the relatively small number of ions in close vicinity to the probe ion. Thus, for the case of three ions distributed at random in a coordination shell of a given radius  $r_s$ , an exact derivation of  $F(D, S)$  can be given, including an exact treatment of the excluded volume (for hard spheres). Since the EFG distribution caused by only three ions is of limited practical interest, we defer the presentation of this calculation to the Appendix. An extension of our approach to  $N_I > 3$  may be possible, and already the case  $N_I = 4$  could be applied to investigations of tetrahedrally coordinated amorphous semiconductors.

### III. AMORPHOUS SOLIDS WITH RANDOM ATOMIC ARRANGEMENTS: AN ANALYTIC APPROXIMATION FOR $P(V_{zz}, \eta)$

#### A. Working definition of a random amorphous solid

Structural models for amorphous metals and alloys with random atomic arrangements are generally based on computer simulations. An analytic expression for the distribution function  $P(V_{zz}, \eta)$  cannot be derived from these models. On the other hand, approaches which are appropriate for random dilute systems such as gases and dilute alloys<sup>28</sup> are not applicable to our problem where the distribution of fields originates from densely packed ionic charges.

For the derivation of  $P(V_{zz}, \eta)$  we have employed a working definition of structural randomness which enables us to overcome these difficulties. We consider the surroundings of the ion containing the probe nucleus as composed of spherical coordination shells, and we define structural randomness by

- (i) random (i.e., uniform except for the excluded volume associated with each ion) distribution of ionic angular positions in any shell, and
- (ii) absence of any correlations between the distributions of ionic charges in different shells.

The results of our general considerations were tested by comparison with the EFG distribution obtained from computer-generated ensembles of spherical shells occupied at random by ionic charges. The results of these computer experiments were employed in particular for an empirical determination of the influence of excluded volumes on the distribution function  $P(V_{zz}, \eta)$ . Most of the computer experiments were carried out following the assumption of spherical shells in the most restrictive sense: The center of all ions was assumed to lie on the surface of a sphere with radius  $r_s$  (the shell radius). Random distributions of ionic angular positions in a shell were obtained by drawing pairs of numbers, interpreted as polar coordinates  $(\cos\theta, \phi)$  in some arbitrary fixed coordinate frame, with help of a random number generator. The ions were treated as hard spheres of radius  $r_I$ , and in the construction of a shell a new ionic position was accepted only if no overlap occurred with any of the ions whose positions had been drawn before. Ensembles of shells were constructed with shell radius  $r_s$  in the range from  $2r_I$  (corresponding to the first coordination shell) up to  $8r_I$ . The number of ions occupying a shell was either restrained to have some constant value  $N_I$ , or alternatively a distribution of oc-

cupation numbers  $N_I$  was obtained by a predetermined number of attempts at finding a new ionic position in a given shell.

The extension of the validity of our results to random ionic arrangements which are not restrained by the partition into spherical shells was tested in computer experiments in which the radial distance of the ions from the probe nucleus was treated as a random variable along with the angular coordinates, up to a range of radii extending from  $2r_I$  to  $6r_I$ .

#### B. The EFG distribution originating from ions in a single spherical shell

##### 1. The contribution of shells with large radius ( $r_s \gg r_I$ )

Let us initially consider the distribution of the quantities  $U_m$  caused by a constant number  $N_I$  of ions, all with the same charge  $q$ , in a single spherical shell with large radius  $r_s \gg r_I$ . Distribution functions arising from ions in a single shell are marked by a superscript (s). A density parameter  $\rho$  is defined by the relation<sup>29</sup>

$$N_I = \frac{2\pi}{\sqrt{3}} (r_s/r_I)^2 \rho. \quad (14)$$

The value of the ratio  $r_s/r_I$  is assumed to be large enough that large values for  $N_I$  are obtained even for  $\rho \ll 1$ . Then excluded-volume effects can be neglected, and the angular coordinates  $(\cos\theta_n, \phi_n)$  of all ions can be treated as independent random variables. According to Eqs. (3) for all  $m$  the quantities  $U_m$  are sums of terms each of which depends upon the position of one ion only:  $U_m = \sum_{n=1}^{N_I} u_m(n)$ . Along with  $(\cos\theta_n, \phi_n)$  the values of the individual terms  $u_m(n)$  are distributed in the finite range  $-q/r_s^3 \leq u_m(n) \leq q/r_s^3$ . Furthermore, for all  $m$  the average value of each term is zero, and its variance is  $\sigma^2[u_m(n)] = q^2/(5r_s^6)$ . Thus, the conditions for application of the central limit theorem<sup>30</sup> are fulfilled, and for sufficiently large  $N_I$  the distribution functions  $P_m^{(s)}(U_m)$  become nearly Gaussian functions:

$$P_m^{(s)}(U_m) \approx \frac{1}{(2\pi)^{1/2} \sigma(r_s, \rho)} \exp\{-U_m^2/[2\sigma^2(r_s, \rho)]\} \quad (15)$$

with

$$\sigma^2(r_s, \rho) = N_I \sigma^2[u_m(n)] = \frac{2\pi}{5\sqrt{3}} \frac{q^2 \rho}{r_s^4 r_I^2} \quad (16)$$

independent of  $m$ .

The distributions of the quantities  $U_m$  obtained from computer experiments are described very well by Gaussians for ensembles of spherical

shells with radius  $r_s \geq 6r_I$  and containing about 30 or more ions at random angular positions. The Gaussian form was found to hold as well for values of the density  $\rho$  extending far beyond the limit  $\rho \ll 1$  imposed above in the derivation of Eq. (15). For this region of higher densities, the following considerations yield an expression for the dependence of the variance  $\sigma(r_s, \rho)$  upon  $\rho$ : For the limit  $\rho=1$ , the limit of a completely full shell,  $\sigma(r_s, \rho=1)=0$  since for a uniform charge distribution all  $U_m$  are zero. Nonuniform charge distributions leading to nonzero values for  $\sigma(r_s, \rho)$  are obtained by removing ions, that is, by introducing "holes" in the shell. Thus, there is a certain analogy between holes and ions which can be accounted for if  $\rho$  in Eq. (16) is replaced by  $\rho(1-\rho)^{1+\alpha}$ . If holes were exactly equivalent to ions,  $\alpha=0$  would be the proper value for  $\alpha$ . In reality, however, there is a difference since in contrast to ions, holes are not quantized entities. They can be finely divided and distributed between the ions. A comparison with the variances  $\sigma^2 = \langle U_m^2 \rangle - \langle U_m \rangle^2$  obtained from computer experiments for several values of  $r_s$  and  $\rho$  (Fig. 1) shows that for  $r_s \geq 6r_I$  the data are quite well reproduced by the relation

$$\sigma^2(r_s, \rho) = \frac{2\pi}{5\sqrt{3}} \frac{q^2 \rho (1-\rho)^{1+\alpha}}{r_s^4 r_I^2} \quad (17)$$

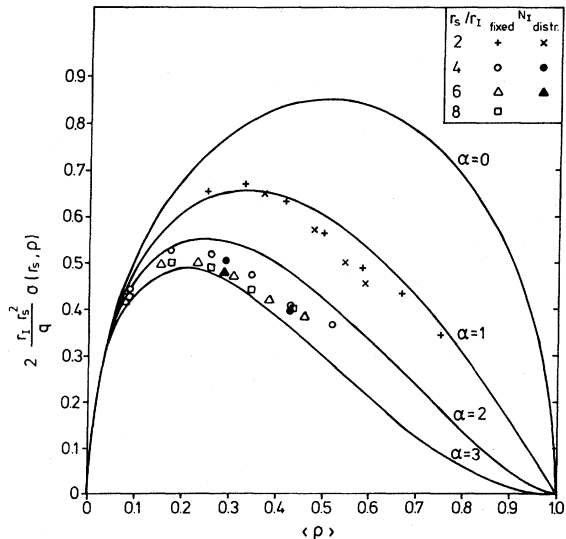


FIG. 1. Dependence of the variance  $\sigma$  upon the density parameter  $\rho$ , defined in Eq. (14) for  $r_s/r_I \geq 4$ . For  $r_s/r_I = 2$ , we have used the appropriate value  $\rho = N_I/12$  (Ref. 29). Results obtained in computer experiments for different values of the ratio  $r_s/r_I$ , either for constant values  $N_I$  or for a distribution of coordination numbers  $N_I$ , are distinguished by different symbols. Continuous curves correspond to Eq. (17) for the values of  $\alpha$  given in the figure.

with  $2 < \alpha < 3$ . For  $r_s < 6r_I$  the computer results for  $\sigma(r_s, \rho)$  increase faster with decreasing  $r_s$  than predicted by Eq. (17). There, of course, we are leaving the region of shell radii for which the central limit theorem is applicable since for  $r_s < 6r_I$  even in the case of a completely filled shell  $N_I$  is not a very large number.

The joint distribution function  $P_u^{(s)}(\dots U_m \dots)$  of all quantities  $U_m$  ( $m=0, \dots, 4$ ) is the product of the functions  $P_m^{(s)}(U_m)$  if the quantities  $U_m$  are independent random variables. For large values of  $N_I$  the condition of independence is approximately fulfilled,<sup>31</sup> and thus in this limit

$$\begin{aligned} P_u^{(s)}(\dots U_m \dots) &\approx \prod_m P_m^{(s)}(U_m) \\ &\approx \frac{1}{(2\pi)^{5/2} \sigma^5} \exp\left(-\sum_m U_m^2 / (2\sigma^2)\right) \\ &\approx \frac{1}{(2\pi)^{5/2} \sigma^5} \exp[-S / (2\sigma^2)]. \quad (18) \end{aligned}$$

Then we obtain by Eq. (10) the distribution function of the splitting parameters  $V_{zz}$  and  $\eta$ :

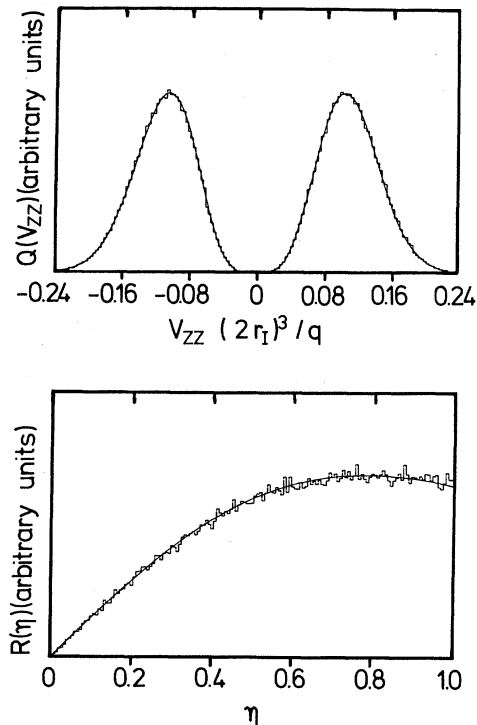


FIG. 2. Marginal distributions  $Q(V_{zz}) = \int_0^1 d\eta P(V_{zz}, \eta)$  and  $R(\eta) = \int_{-\infty}^{\infty} dV_{zz} P(V_{zz}, \eta)$  for the Gaussian approximation, Eq. (19), for  $P(V_{zz}, \eta)$ . The functions corresponding to Eq. (19) (solid lines) are compared with the results obtained from a computer experiment for an ensemble of shells with radius  $r_s = 6r_I$ , randomly occupied by  $N_I = 30$  ions.

$$P^{(s)}(V_{zz}, \eta) = \frac{1}{(2\pi)^{1/2} \sigma^5} V_{zz}^4 \eta (1 - \eta^2/9) \times \exp[-V_{zz}^2(1 + \eta^2/3)/(2\sigma^2)]. \quad (19)$$

In Fig. 2 the marginal distributions  $Q(V_{zz}) = \int d\eta P(V_{zz}, \eta)$  and  $R(\eta) = \int dV_{zz} P(V_{zz}, \eta)$  derived from Eq. (19) are shown in comparison with the results of a computer experiment for an ensemble of shells with radius  $r_s = 6r_I$ , randomly occupied by  $N_I = 30$  ions. The value substituted in Eq. (19) for the parameter  $\sigma$  was the computer result for the variance of the quantities  $U_m$ .

## 2. The contribution of nearby coordination shells

The most remarkable feature of the distribution function  $P^{(s)}(V_{zz}, \eta)$  obtained for computer-generated ensembles of shells containing a small number of ions is a pronounced asymmetry with respect to the sign of  $V_{zz}$  (Fig. 3).

The physical origin of this asymmetry is easily

recognized: The sign of  $V_{zz}$  depends both on the sign of the charges causing the EFG and on their spatial arrangement. For a metallic solid we suppose the ions to carry a positive charge. Then the largest positive value of  $V_{zz}$  ( $N_I q r_s^{-3}$  for  $N_I$  ions of zero radius) results when all ions are clustered near a single point or else near two points at the opposite poles of a diameter of the shell whereas the largest negative value ( $-\frac{1}{2} N_I q r_s^{-3}$ ) is obtained when the ions form a ring (around the equator of the shell, say) with approximately equal interionic spacings. Apart from the large numerical difference between the extreme positive and negative values, the two configurations have completely different characters, and different probability densities for configurations giving rise to positive or negative values of  $V_{zz}$ , respectively, may be expected. This asymmetry is strongly affected by excluded volumes. For the case of six hard-sphere ions in the first coordination shell ( $r_s/r_I = 2$ ), for example, the

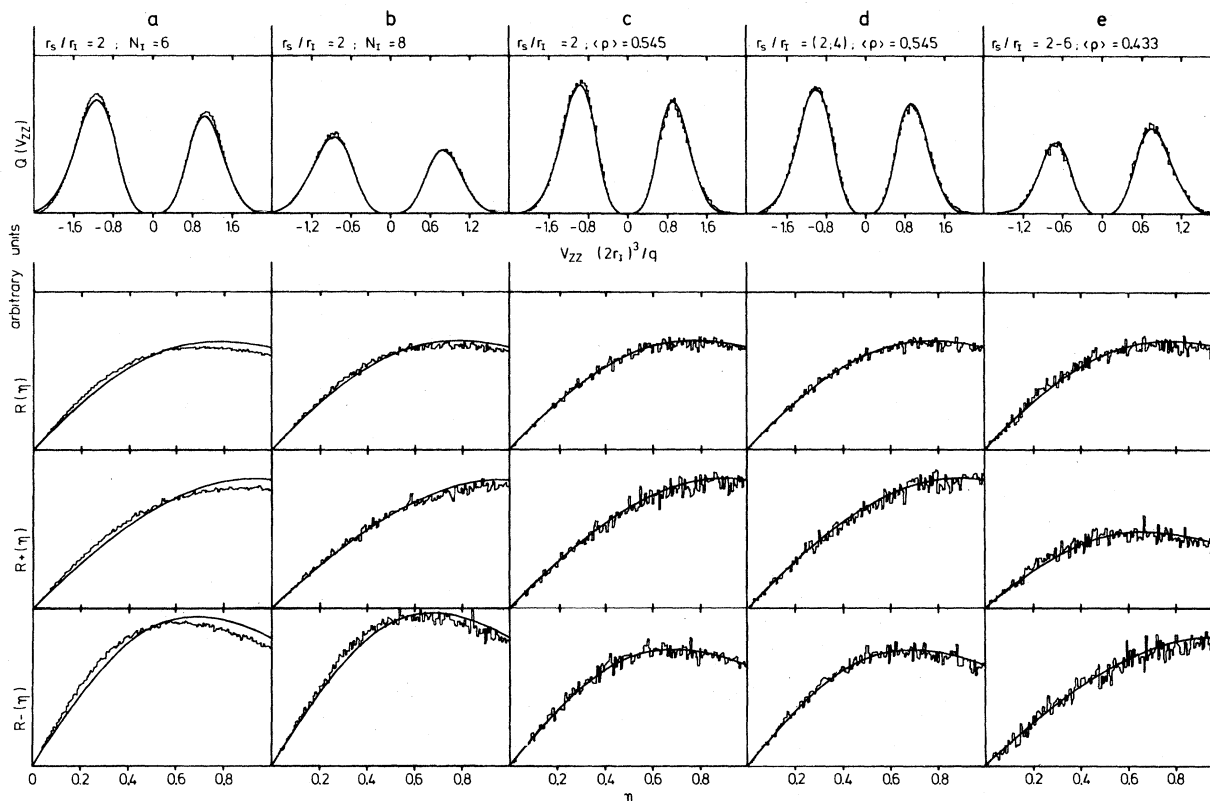


FIG. 3. Marginal distributions  $Q(V_{zz})$ ,  $R(\eta)$ ,  $R_+(\eta)$  (integration only over positive  $V_{zz}$ ), and  $R_-(\eta)$  (only negative  $V_{zz}$ ) for ensembles of shells containing a small number  $N_I$  of ions. For (a) and (b), the values of  $N_I$  are shown above the figure. For (c), the distribution of coordination numbers  $N_I$  is shown in Fig. 5. Average densities  $\langle \rho \rangle$  correspond to the definition  $N_I = 3(r_s/r_I)^2 \rho$ , appropriate for  $r_s/r_I = 2$ . (d) shows the result obtained for independent distributions of charged ions in two shells with radii  $r_s = 2r_I$  and  $r_s = 4r_I$ . For (e), the radial distance of the ions was a random variable in the range from  $2r_I$  to  $6r_I$ . The continuous curves are derived from Eq. (21) with values for the parameters  $\sigma$  and  $\beta$  obtained from least-squares fits to the computer-generated data for  $Q(V_{zz})$ ,  $R_+(\eta)$ , and  $R_-(\eta)$ .

largest positive value of  $V_{zz}$  is only  $3qr_s^{-3}$ , equal in magnitude to the largest value for negative  $V_{zz}$ .

When the distribution function is expressed in terms of the invariant functions  $D$  and  $S$  of the tensor components, the asymmetry is reflected in the dependence of  $F(D, S)$  upon  $D$ : The sign of  $D$  is the same as that of  $V_{zz}$ , whereas  $S$  is an even function of  $V_{zz}$ . Thus, we have analyzed the dependence of the ratio

$$A(S, D) = [F(D, S) - F(-D, S)] / [F(D, S) + F(-D, S)],$$

derived from computer-generated distribution functions, upon  $D$  and  $S$  in order to find an appropriate

approximation for the asymmetry. For  $N_I = 4$  and  $N_I = 5$  the results indicate a rather complex dependence of  $A(S, D)$  on both variables. For  $N_I \geq 6$ , however,  $A(S, D)$  is proportional to  $D$  for a large range of values of the variables (Fig. 4). Furthermore, for ions in the first coordination shell ( $r_s/r_l = 2$ ), the dependence of  $A$  upon  $S$  is negligible. In this case we can write  $A(S, D) = aD$  with constant  $a$ .

Apart from this asymmetry, all features of the distribution functions shown in Fig. 3 are essentially the same as those of the Gaussian approximation (Fig. 2). Thus we combine the result ob-

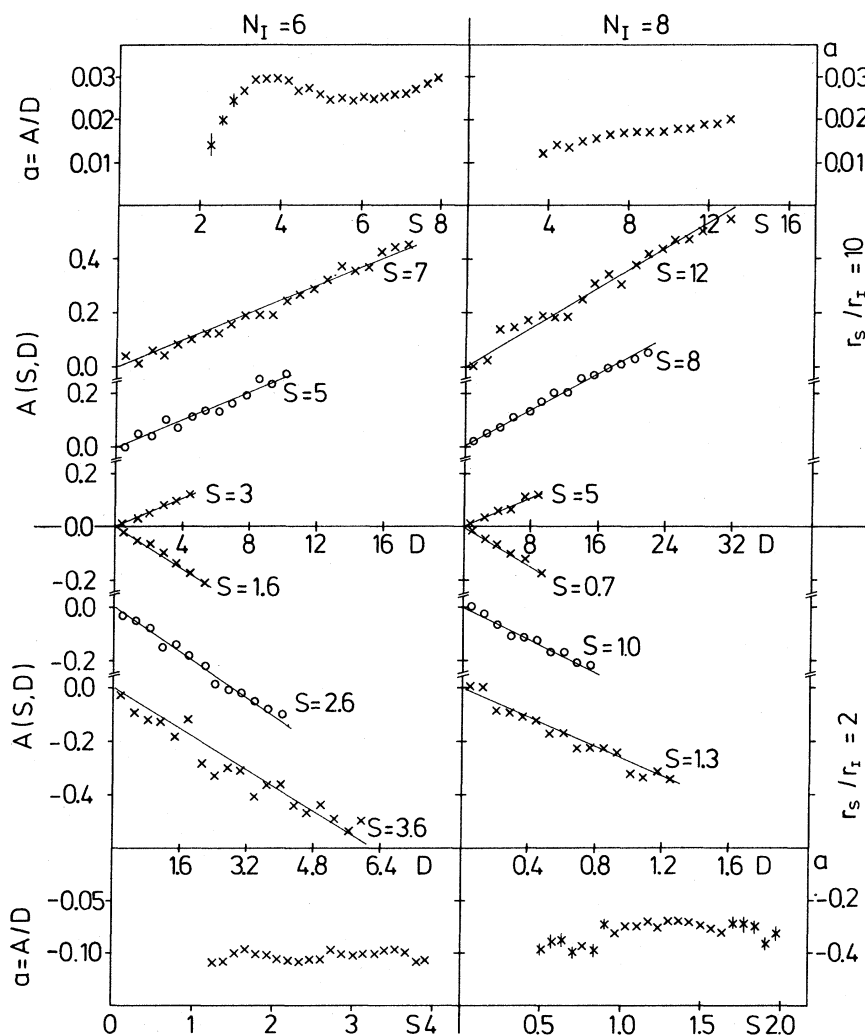


FIG. 4. Analysis of the asymmetric part  $A(S, D)$  of the distribution function  $F(D, S)$ , defined by  $A(S, D) = [F(D, S) - F(-D, S)] / [F(D, S) + F(-D, S)]$ , obtained for ensembles containing  $N_I = 6$  (left-hand side) and  $N_I = 8$  (right-hand side) ions, respectively. The upper part of the figure refers to  $r_s/r_l = 10$ , the lower part to  $r_s/r_l = 2$ . Values for  $S$  are given in units  $(q/r_s^3)^2$ , for  $D$  the unit is  $(q/r_s^3)^3$ . In the center the dependence of  $A(S, D)$  upon  $D$  for a few values of  $S$  is shown. As indicated, the computer-results are well reproduced by straight lines,  $A(S, D) = a(S)D$ . Above and below, the dependence of the slopes  $a(S)$  upon  $S$  is displayed.



tained for  $A(S, D)$  with the Gaussian expression, Eq. (18), for the symmetric part of the distribution function,  $[F(D, S) + F(-D, S)]/2$ , and the contribution of nearby coordination shells containing at least six ions to the EFG distribution is approximated by

$$F^{(s)}(D, S) = \frac{1}{6(2\pi)^{1/2}\sigma^3} (1 + \beta D/\sigma^3) \exp[-S/(2\sigma^2)]. \quad (20)$$

With this notation,  $\beta$  is a dimensionless parameter. Equation (20) cannot be valid for arbitrarily large values of  $D$  since  $F^{(s)}(D, S)$  becomes negative when  $\beta D/\sigma^3 < -1$ . This problem could be solved by the introduction of terms proportional to  $D^2$  and higher powers of  $D$  such that  $F^{(s)}(D, S)$  becomes positive definite. Such terms, however, entail the introduction of additional parameters. We see at the moment no possibility for a rigorous derivation of their values. Therefore, we have chosen the alternative approach of setting the second term to zero for values of  $D$  outside the range  $-\sigma^3/|\beta| \leq D \leq \sigma^3/|\beta|$ . For the cases of practical interest this range is large compared to the width of the distribution, and the fraction of the ensembles affected by the cutoff is quite small.

In this approximation the distribution function for the splitting parameters  $V_{zz}$  and  $\eta$  is given by

$$P^{(s)}(V_{zz}, \eta) = \frac{V_{zz}^4 \eta}{(2\pi)^{1/2} \sigma^3} (1 - \eta^2/9) [1 + \beta V_{zz}^3 (1 - \eta^2)/\sigma^3] \times \exp[-V_{zz}^2 (1 + \eta^2/3)/(2\sigma^2)]. \quad (21)$$

In accordance with the prescription given above for the expression in terms of  $D$  and  $S$ , we set the second term equal to zero when  $|\beta V_{zz}^3 (1 - \eta^2)/\sigma^3| > 1$ . As shown in Figs. 3(a) and 3(b), Eq. (21) with parameter values  $\sigma$  and  $\beta$  derived from a least-squares fit to the marginal distribution functions  $Q(V_{zz})$ ,  $R_+(\eta)$  and  $R_-(\eta)$  (Ref. 32) reproduces qualitatively the features of the distribution function obtained from computer experiments for rather small values  $N_I$ . Deviations in quantitative details decrease with increasing values  $N_I$ .

According to the structural models for randomly coordinated amorphous solids, however, some distribution of coordination numbers  $N_I$  can be expected.<sup>33</sup> Computer experiments in which ensembles of spherical shells with variable  $N_I$  were produced by the procedure outlined in Sec. III A yielded distribution functions of the splitting parameters which are very well approximated by Eq. (21). This is demonstrated in Fig. 3(c) by the results obtained for an ensemble of shells with the distribution of coordination numbers  $N_I$  shown in Fig. 5.

The values of  $\beta$  obtained by least-squares fits of Eq. (21) to the computer-generated distributions depend both on the shell radius  $r_s$  and on the density  $\rho$ . At low densities ( $\rho \leq 0.3$ ) which are hardly of practical interest, positive values of  $\beta$  are obtained for all values of  $r_s$ , up to  $\beta \sim 0.03$  for  $\rho \sim 0.1$ , the lowest density considered. For  $\rho \geq 0.4$ , however,  $\beta$  has negative values which are nearly independent of the density. For the shell radius  $r_s = 2r_I$ , corresponding to the first coordination shell,  $\beta \sim -0.02$  at these densities. With increasing  $r_s$ ,  $|\beta|$  decreases rapidly, and for  $r_s \sim 6r_I$ , the experimental distribution functions are very well approximated by the Gaussian approximation, Eq. (19), corresponding to  $\beta = 0$ .

### C. The EFG distribution for a random amorphous solid

Having established an approximate expression for the distribution function  $P^{(s)}(V_{zz}, \eta)$  caused by ions randomly arranged in a single spherical shell we are now left with the task of finding the EFG distribution due to all ionic charges surrounding the probe nuclei. According to proposition (ii) of our working definition of a random amorphous solid given in Sec. III A the distribution function of the quantities  $U_m$  caused by the entire environment is obtained by folding the distribution functions  $P_u^{(s)}(\dots U_m \dots)$  arising from the spherical shells with different radii  $r_s$ .

The folding operation is easily performed by Fourier transformation of the function  $P_u^{(s)}(\dots U_m \dots)$  if the cutoff of the asymmetric term proportional to  $D$  for large values of  $D$  is neglected. In view of the approximate nature of Eq. (21), and since the total contribution of the region affected by the cutoff is small, this neglect should not seriously impair the final outcome. Similarly, in the Fourier transform of the folded distribution function, terms involving products  $\beta_{s_1} \beta_{s_2} \dots$  (different indices  $s_1, s_2, \dots$  refer to

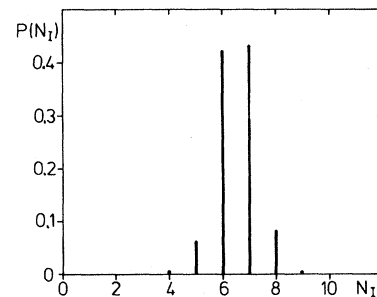


FIG. 5. Distribution of coordination numbers  $N_I$  for the ensemble for which the results shown in Fig. 3(c) were obtained.

different coordination shells) of second and higher order are neglected. This is justified by the small value of  $\beta$  even for the first coordination shell and by the rapid decrease of  $\beta_s$  to zero with increasing shell radius  $r_s$ .

The resulting approximation for the EFG distribution in a random amorphous solid is given by the same expression as the contribution due to a single shell:

$$P(V_{zz}, \eta) \approx \frac{V_{zz}^4 \eta}{(2\pi)^{1/2} \sigma^5} (1 - \eta^2/9) [1 + \beta V_{zz}^3 (1 - \eta^2)/\sigma^3] \times \exp[-V_{zz}^2 (1 + \eta^2/3)/(2\sigma^2)] \quad (22)$$

with parameters

$$\sigma = \left( \sum_s \sigma_s^2 \right)^{1/2}, \quad \beta = \sum_s (\beta_s \sigma_s^3) / \sigma^3. \quad (23)$$

The rapid decrease of  $\sigma_s$  and of  $\beta_s$  with  $r_s$  guarantees the convergence of both sums to a finite value. Actually, the final result is strongly dominated by the contribution of the first coordination shell which amounts to more than 80% of the final value for  $\sigma$ , over 90% for  $\beta$ .

We have tested the validity of our approach by computer experiments in which random ionic arrangements in two and three shells with radii  $r_s = 2r_I$ ,  $4r_I$ , and  $6r_I$  were generated such that the average density was the same in all shells. The results show that the approximation of Eq. (22) to the distribution functions in these cases is at least as good as to those due to a single shell. As an example we display in Fig. 3(d) the distribution function obtained for two shells with radii  $r_s = 2r_I$  and  $r_s = 4r_I$ . The average density was the same as for the ensemble for which the results are shown in Fig. 3(c). The similarity of Figs. 3(c) and 3(d) demonstrates the dominant role of the first shell for the EFG distribution in a random amorphous solid.

At this point the question arises to what extent these results are influenced by the restrictions imposed by our definition of a random amorphous solid, in particular by the strict partition of the ionic distribution into spherical shells. We have tested this question empirically by computer-generated ensembles of ionic environments in which both angular and radial coordinates of the ions were distributed at random. The result is illustrated in Fig. 3(e) by the distribution function obtained for an ensemble in which the radial positions of the ions varied at random in the range from  $2r_I$  to  $6r_I$ . This distribution is very well approximated by an expression as given by Eq. (22), but the parameter values differ considerably from those obtained for ionic distributions of comparable densities with a partition into spherical

shells. For the unpartitioned ionic distribution, in particular, the sign of  $\beta$  is inverted. As we have pointed out in the Introduction, the parameter values (including the sign of  $\beta$ ), derived here in the framework of a point-charge calculation, are not likely to be realistic anyway. The essential result of our work is the functional form of the EFG distribution, and we conclude from the outcome of these unrestricted computer experiments that this result is valid beyond the restriction imposed by our working definition of a random amorphous solid.

In our derivation of the distribution function  $P(V_{zz}, \eta)$  we have assumed all ions to carry the same charge. This assumption is appropriate for a monoatomic amorphous material. However, the same functional expression can be expected to approximate the EFG distribution in random amorphous alloys, except in the limit of high dilution. In the expressions Eq. (3) for the parameters  $U_m$  in terms of the charges and their coordinates the charges  $q_n$  and the radial coordinates  $r_n$  occur only in the combination  $(q_n/r_n^3)$ . Thus, variations of the charges are essentially equivalent to variations of radial distances which according to the results of the computer experiments do not modify the form of the distribution function.

If the concentration of one alloy component is very low, however, the large probability of finding only one or two ions of this component in the first coordination shell leads to singular features in the EFG distribution which will therefore deviate significantly from the smooth distribution function originating from random charge distributions at higher densities.

The results obtained by Pustówka *et al.*<sup>34</sup> in calculating the EFG distribution in random binary crystalline alloys (bcc, fcc, and hcp lattice), that is for the case of purely chemical disorder, fully support these arguments. The distribution functions of the splitting parameter  $\Delta = V_{zz}(1 + \eta^2/3)^{1/2}$  calculated by these authors for alloy concentrations  $c$  in the range  $0.2 \leq c \leq 0.8$  are quite similar to those derived in the present work for the case of structural disorder in a pure material.

#### IV. MÖSSBAUER SPECTRA OF <sup>155</sup>Gd IN AMORPHOUS Gd-Ni ALLOYS

The assumption of a random distribution of ionic charges underlying the derivation of the distribution function  $P(V_{zz}, \eta)$  in Sec. III corresponds in its essential traits to DRPHS-type models of amorphous metallic solids. This is demonstrated by the similarity of the distributions shown in Figs. 2 and 3 with those derived by computer simulations of DRPHS structures for the EFG

distribution<sup>7-9</sup> and for crystal-field splittings.<sup>13</sup> Thus, a comparison of nuclear quadrupole splittings observed by NMR or Mössbauer spectroscopy with the expression given in Eq. (22) provides an experimental test regarding the validity of DRPHS-type structural models. Investigations of this kind are of particular interest for amorphous rare-earth alloys in view of the consequences of the crystal-field distribution for the magnetic properties of these materials.

With this objective we have analyzed Mössbauer absorption spectra of <sup>155</sup>Gd in amorphous Gd-Ni alloys. For investigations of the EFG distribution in amorphous rare-earth alloys by Mössbauer spectroscopy, Gd is well suited as a probe since the ground state of the Gd 4f shell is an S state which does not contribute to the EFG. Thus, the observed quadrupole splitting is caused entirely by the distribution of charges outside the electronic shell localized at the probe nuclei. The nuclear properties of <sup>155</sup>Gd are less favorable. The quadrupole moment of the nuclear ground state (Ref. 35),  $Q_g = (1.59 \pm 0.15) \times 10^{-24}$  cm<sup>2</sup>, is large, but for its spin  $I_g = \frac{3}{2}$  the quadrupole splitting is completely determined by the absolute value of the single parameter  $\Delta = V_{zz}(1 + \eta^2/3)^{1/2}$ . The quadrupole moment of the excited state<sup>36</sup> with spin  $I_e = \frac{5}{2}$ ,  $Q_e = (0.14 \pm 0.02) \times 10^{-24}$  cm<sup>2</sup>, is small, and the quadrupole splitting of the excited state is mostly unresolved. Thus, in the absence of a magnetic hyperfine field the Mössbauer spectrum of <sup>155</sup>Gd is neither sensitive to the sign of  $V_{zz}$  nor to the asymmetry parameter  $\eta$ .

More details about the distribution function  $P(V_{zz}, \eta)$  can be deduced from Mössbauer spectra in magnetically ordered samples. In this case, the dependence of the nuclear energy levels upon the direction of the magnetic hyperfine field with respect to the principal axes of the EFG tensor has to be accounted for. In an isotropic amorphous material with perfect ferromagnetic alignment these directions are distributed isotropically. In a real amorphous ferromagnet, however, the alignment may not be perfect,<sup>37</sup> and thus the isotropy of the distribution is not guaranteed. This uncertainty is removed when spectra are taken with absorbers in an applied magnetic field of sufficient strength, provided the material is structurally isotropic. For our samples at 4.2 K the magnetization was found to be saturated in fields above 1.5 tesla when the direction of the field was perpendicular to the plane of the platelike samples as in our Mössbauer spectrometer. Thus, for spectra taken in larger fields we can assume the magnetic hyperfine field to have the same direction as the external magnetic field which was applied parallel to the direction of observation.

Mössbauer absorption spectra were taken of amorphous samples of composition Gd<sub>0.2</sub>Ni<sub>0.8</sub> and Gd<sub>0.4</sub>Ni<sub>0.6</sub>, prepared by sputtering onto a substrate which was cooled to 77 K. Details concerning the techniques employed in taking <sup>155</sup>Gd Mössbauer spectra have been described previously.<sup>38</sup> In this paper we only present results which are related to the EFG distribution. Results of interest for the magnetic properties of these alloys are deferred to a separate publication.

Examples for <sup>155</sup>Gd Mössbauer spectra obtained with the absorber of composition Gd<sub>0.4</sub>Ni<sub>0.6</sub> are displayed in Fig. 6, with Gd<sub>0.2</sub>Ni<sub>0.8</sub> in Fig. 7. For the spectra shown in Figs. 6(a) and 7(a) the absorber temperature was 70 K, for both samples above the Curie temperature. For Gd<sub>0.2</sub>Ni<sub>0.8</sub>,  $T_c = (39 \pm 1)$  K and for Gd<sub>0.4</sub>Ni<sub>0.6</sub>,  $T_c = (63 \pm 2)$  K was determined by magnetization measurements. The information content of these spectra is very limited, partly because of the values of nuclear spins and quadrupole moments quoted above, but also because of the very small absorption cross section at this temperature. Due to their simplicity, however, they were useful for confirming the average value of  $V_{zz}$  since the value deduced from the spectra obtained at lower temperatures may be subject to doubt in view of the simultaneous presence of magnetic dipole and electric quadrupole interactions of similar strength. Both spectra are adequately described if we assume a unique value for  $V_{zz}$ , but a broadened width of the absorption lines  $\Gamma_A \approx 0.8$  mm/sec instead of the natural width  $\Gamma_0 = 0.25$  mm/sec. The additional width  $\delta\Gamma = \Gamma_A - \Gamma_0 \approx 0.55$  mm/sec amounts to about 30% of the average ground-state quadrupole splitting. This result already indicates the presence of some distribution of electric field gradients. Variations of the isomer shift presumably contribute to the line broadening, but only a small fraction of the observed width should arise from isomer shift variations since the total shift between GdNi<sub>5</sub> and pure Gd amounts to 0.22 mm/sec.<sup>39</sup>

As illustrated by Fig. 6(f), the assumption of a unique value for  $V_{zz}$  does not describe the spectra obtained at 4.2 K. In this figure we show the result for the assumptions  $V_{zz} > 0$  and  $\eta = 0$  only. Similar misfits were obtained for a negative value of  $V_{zz}$  and for a nonzero value of  $\eta$ . All spectra taken at 4.2 K, however, could be fitted with an EFG distribution as given by Eq. (22). The best agreement with the experimental data resulted consistently for all spectra from fits with  $\beta = 0$  and with a linewidth  $\Gamma_A = 0.34$  mm/sec, slightly larger than  $\Gamma_0$ . The results of least-squares fits with this model are shown in Figs. 6(a)–6(e) as solid lines.

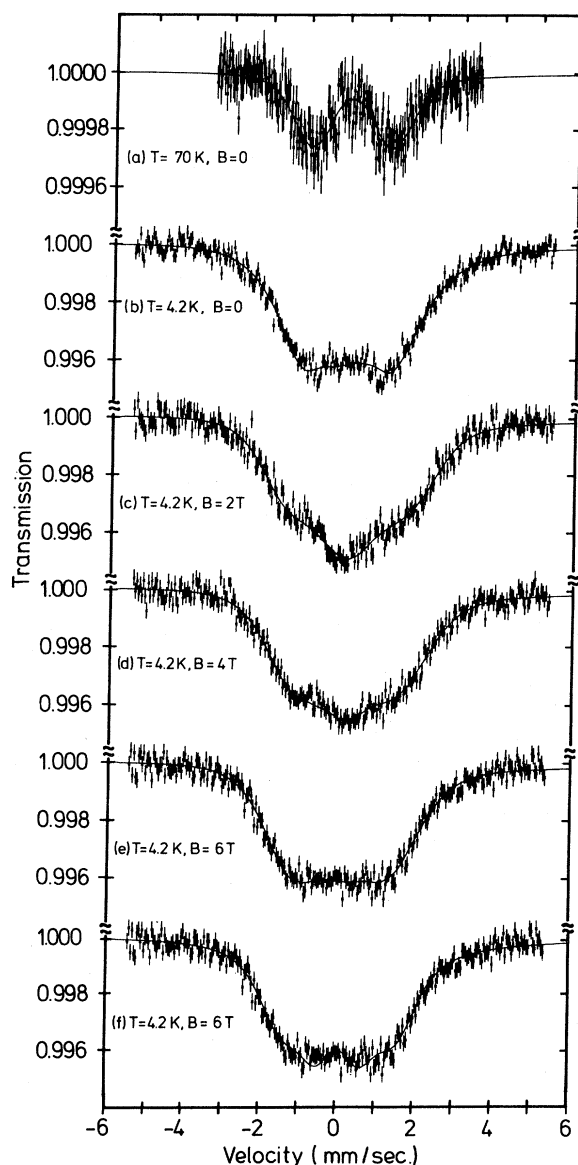


FIG. 6. Mössbauer absorption spectra of  $^{155}\text{Gd}$  in amorphous  $\text{Gd}_{0.4}\text{Ni}_{0.6}$ . Absorber temperatures  $T$  and values of the applied field  $B$  are given in the figure. Solid lines in (a)–(e) were obtained from least-squares fits with an EFG distribution given by Eq. (22) with  $\beta=0$ . The curve in (f) is the result of a least-squares fit with the assumption of a unique value for  $V_{zz}$ .

The spectra obtained for  $\text{Gd}_{0.2}\text{Ni}_{0.8}$  at 4.2 K are neither described by the assumption of a unique value of  $V_{zz}$  nor by the distribution function given in Eq. (22) [Fig. 7(e)]. This failure is understandable if nickel ions in these alloys carry no or only a very small charge such that the EFG is determined by the distribution of Gd ions. Zero effective charge on nickel ions will result if the

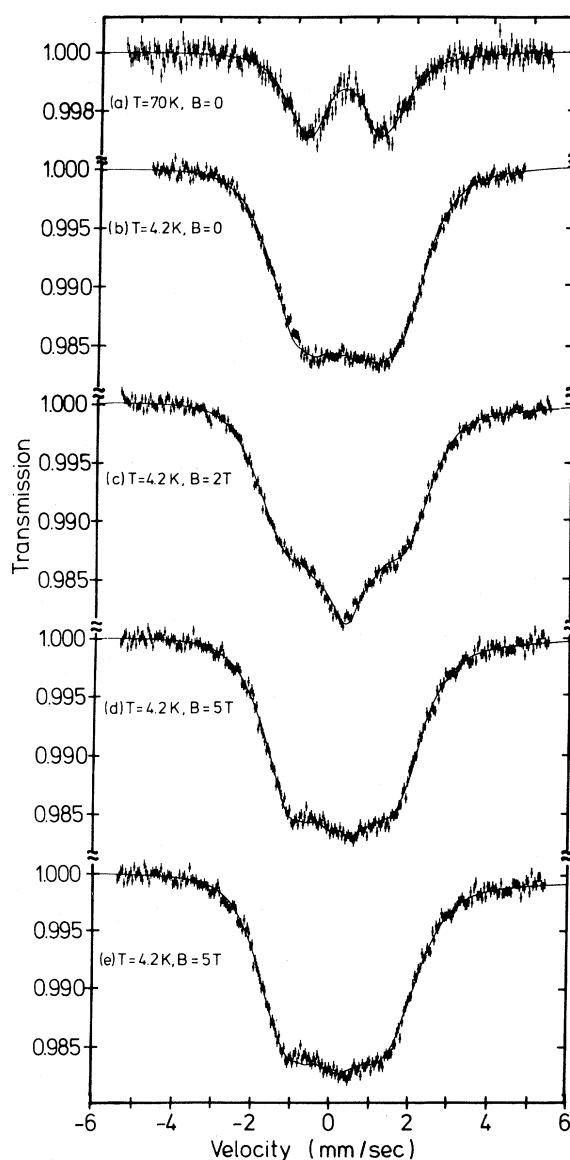


FIG. 7. Mössbauer absorption spectra of  $^{155}\text{Gd}$  in amorphous  $\text{Gd}_{0.2}\text{Ni}_{0.8}$ . Solid lines in (a)–(d) were obtained from least-squares fits with an EFG distribution  $P(V_{zz}, \eta) = 0.71P_2(V_{zz}, \eta) + 0.29P_3(V_{zz}, \eta)$  with distribution functions  $P_{N_I}(V_{zz}, \eta)$  corresponding to Gd nuclei with  $N_I = 2$  and  $N_I = 3$  Gd neighbors, respectively, assuming the charge of Ni ions to be negligible. The functions  $P_{N_I}(V_{zz}, \eta)$  are described in the Appendix. The curve in (e) is the result of a least-squares fit with the EFG distribution given by Eq. (22).

$3d$  band is completely filled as may be expected since x-ray induced photoelectron spectra have shown the  $3d$  band in amorphous alloys containing  $3d$  transition metals to be shifted well below the Fermi energy.<sup>40</sup> Filling of the  $3d$  band implies zero magnetic moment for the

nickel ions, in agreement both with the saturation magnetization of our samples and with results of  $^{61}\text{Ni}$  Mössbauer spectra.

At the low Gd concentration of this sample, only a small number of Gd ions will be found in the first coordination shell of the probe ions,<sup>1</sup> and we can not expect Eq. (22) to be a good approximation for the EFG distribution. These spectra were fitted successfully with a distribution function  $P(V_{zz}, \eta)$  composed of our results for two and three ions distributed at random in the first coordination shell (Figs. 8 and 9), that is  $P(V_{zz}, \eta) = a_2 P_2(V_{zz}, \eta) + a_3 P_3(V_{zz}, \eta)$  with  $a_2 + a_3 = 1$ . A least-squares fit to the spectrum shown in Fig. 7(d) yielded the value  $a_2 = 0.71 \pm 0.07$ . The spectra shown in Figs. 7(a)–7(c) were then fitted with this value for  $a_2$ . For the other parameters, the following assumptions were involved in our fitting model: different isomer shifts for  $^{155}\text{Gd}$  nuclei having two or three Gd neighbors, respectively; linewidth  $\Gamma_A = \Gamma_0 = 0.25$  mm/sec.

The EFG distributions which were fitted to these spectra are completely determined by a single parameter. For  $\text{Gd}_{0.4}\text{Ni}_{0.6}$ , since we found  $\beta = 0$ , only the value of the parameter  $\sigma$  remained as an adjustable variable. The result derived

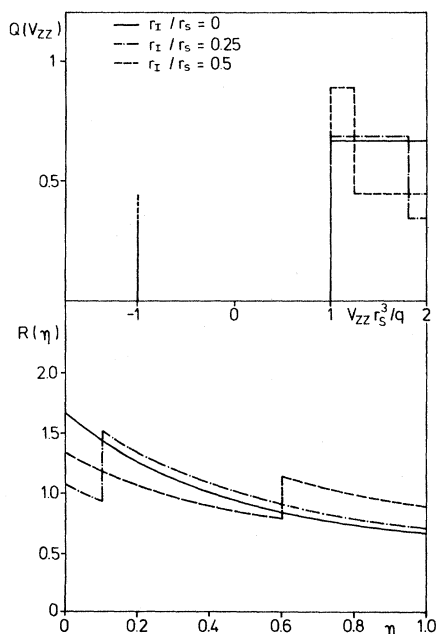


FIG. 8. Marginal distribution functions  $Q(V_{zz})$  and  $R(\eta)$  for the EFG distribution  $P_2(V_{zz}, \eta)$  originating from an ensemble of spherical coordination shells which contain  $N_I = 2$  charged ions with random angular positions. The relative weight associated with the  $\delta$ -function singularity at  $V_{zz} = -q/r_s^3$  in  $Q(V_{zz})$  is indicated by the length of the vertical line at this point.

from the four spectra taken at 4.2 K [including the Sternheimer factor  $(1 - \gamma_\infty)$ ] was  $\sigma = (4.1 \pm 0.1) \times 10^{17}$  V/cm<sup>2</sup>. Similarly, for  $\text{Gd}_{0.2}\text{Ni}_{0.8}$ , once the probabilities of finding two or three Gd ions, respectively, in the first coordination shell were determined, only one scale factor for the  $V_{zz}$  values remained open. We used the EFG caused by a single Gd ion in the first coordination shell,  $V_1$ , as variable scale factor. The fit result was  $V_1^{\text{expt}} = (1 - \gamma_\infty)q_{\text{eff}}/(2r_{\text{Gd}})^3 = (6.6 \pm 0.2) \times 10^{17}$  V/cm<sup>2</sup>.

The ratio between these two experimental results,  $\sigma/V_1^{\text{expt}} = 0.62 \pm 0.02$ , is close to that predicted by our calculations for the concentration dependence of  $\sigma$ , as can be seen by comparison with Fig. 1 where the contribution of the first coordination shell to  $\sigma$  is given in units of the single-ion contribution. Furthermore, these results are surprisingly close to the point-charge value  $V_1^{\text{pc}} = 8.8 \times 10^{17}$  V/cm<sup>2</sup>, calculated with the assumptions  $r_{\text{Gd}} = 1.7 \times 10^{-8}$  cm,  $(1 - \gamma_\infty) = 80$ , and  $q_{\text{Gd}} = 3e = 4.8 \times 10^{-19}$  C.

From our results we can derive an estimate for the average crystal-field term  $\langle D \rangle J_e^2$  acting on rare-earth ions with nonzero orbital angular momentum in analogous alloys. The value of  $\langle D \rangle$  is directly related to the average  $\langle |V_{zz}| \rangle$ :

$$\langle D \rangle = \frac{3}{4} |\alpha_J| \langle r^2 \rangle_{4f} e \langle |V_{zz}| \rangle (1 - \sigma_2)/(1 - \gamma_\infty).$$

For the distribution function  $P(V_{zz}, \eta)$  fitted to the spectra of  $\text{Gd}_{0.4}\text{Ni}_{0.6}$ ,

$$\langle |V_{zz}| \rangle = \frac{5}{(2\pi)^{1/2}} \sigma = (8.2 \pm 0.2) \times 10^{17} \text{ V/cm}^2.$$

A direct comparison is possible with experimental data for amorphous Dy-Ni alloys.<sup>41</sup> The appropriate parameter values for Dy are the following<sup>42,43</sup>:  $\alpha_J = -6.35 \times 10^{-3}$ ,  $\langle r^2 \rangle_{4f} = 2 \times 10^{-17}$  cm<sup>2</sup>. For the ratio  $(1 - \sigma_2)/(1 - \gamma_\infty)$  we use the value  $5 \times 10^{-3}$  given by Dunlap *et al.*<sup>44</sup> Then we obtain  $\langle D \rangle/k_B = 6$  K, in excellent agreement with the value derived by Rebouillat *et al.*,<sup>41</sup> interpreting their magnetization data in terms of the random anisotropy model for amorphous  $\text{DyNi}_3$ .

## V. SUMMARY AND CONCLUSIONS

The atomic structure of an amorphous solid can be determined most completely by combined investigations employing three types of experimental methods.

- (i) Neutron and/or x-ray diffraction which yields radial pair correlation functions,
- (ii) EXAFS for more specific information about short-range atomic coordination numbers and radial distances, and
- (iii) NMR, Mössbauer spectroscopy, or perturbed angular correlation measurements for in-

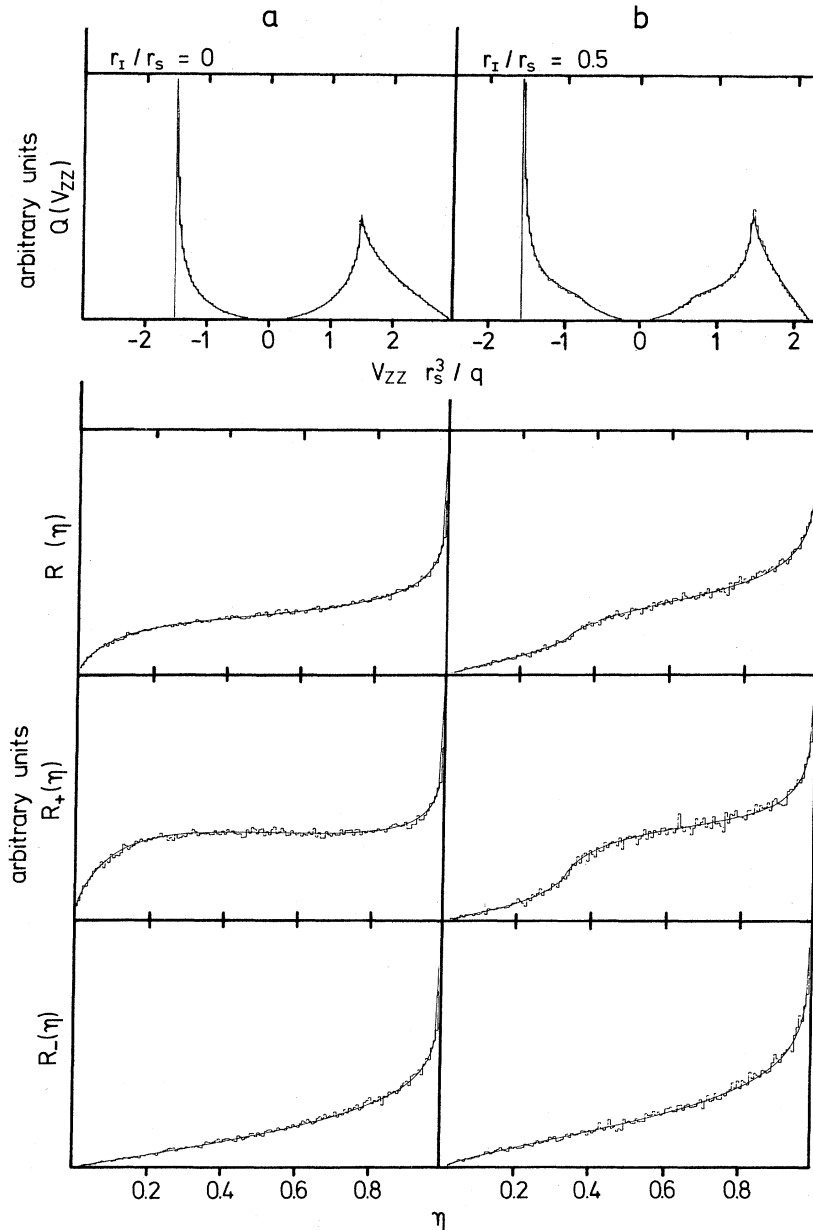


FIG. 9. Marginal distribution functions  $Q(V_{zz})$ ,  $R(\eta)$ ,  $R_+(\eta)$ , and  $R_-(\eta)$  for the EFG distribution  $P_3(V_{zz}, \eta)$  originating from an ensemble of spherical shells which contain  $N_I=3$  charged ions with random angular coordinates. The results of the calculations described in the text, shown by continuous curves, are compared with computer-generated data.

formation about directional distributions of atomic coordination.

The interpretation of results obtained by methods of type (i) and (ii) is well established. However, direct experimental information about directional ionic distributions can be deduced only<sup>45</sup> from distributions of nuclear quadrupole splittings, observable by one of the methods of the third type. Until now, investigations of the relation between

this distribution and the underlying spatial arrangement of ionic charges have been rather rudimentary. In the present paper we describe a first systematic attack at this problem.

For the case of random ionic arrangements, exemplified by DRPHS-type structural models of amorphous metals and alloys, we have derived an approximate formula for the distribution function  $P(V_{zz}, \eta)$  which determines the distribution of

nuclear energy levels. The derivation has been based on two approximations: a hard-sphere model for the ions and point-charge calculations of the EFG. We have presented arguments in support of our approach, showing that the shortcomings of the second approximation do not seriously impair the essential result of our work which is the *form* of the distribution function rather than numerical values of parameters appearing in this function.

The distribution function  $P(V_{zz}, \eta)$  is strongly dominated by the contribution of the first coordination shell. It is characterized by a deep hole in the distribution of  $V_{zz}$  around the value  $V_{zz} = 0$  and by zero probability for  $\eta = 0$ . In general, the probability distribution is not symmetric with respect to the sign of  $V_{zz}$ , i.e.,  $P(-V_{zz}, \eta) \neq P(V_{zz}, \eta)$ . Consequently, the average value of  $V_{zz}$  in general is different from zero. In other words, *there is a rather well defined quadrupole splitting of nuclear energy levels in random amorphous solids, and the interaction will usually have a preferred sign.*

For a more general class of amorphous solids, characterized by overall isotropy, the task of finding the distribution function which in general depends upon five independent variables which determine the EFG tensor, is simplified. The condition of overall isotropy implies that the distribution function depends upon two variables only, the invariant functions  $S$  and  $D$  of the tensor components. Expressions for these invariants in terms of the radial distances of the ionic charges causing the EFG and of the bond angles between pairs of ions, again in the framework of a point-charge model, are given. These expressions for  $S$  and  $D$  may be useful for an exact derivation of the EFG distribution caused by the small number  $N_I$  of ions in the first coordination shell of the probe nuclei. For  $N_I = 3$  we have carried through this derivation. This case is not yet of practical interest, but if our approach could be extended to  $N_I = 4$ , an immediate application to investigations of tetrahedrally coordinated semiconductors would be possible.

We have applied the distribution function  $P(V_{zz}, \eta)$  which we have derived for solids with random ionic arrangement to the analysis of  $^{155}\text{Gd}$  Mössbauer spectra of amorphous Gd-Ni alloys. Although all experimental spectra could be reproduced in this way, we can not yet claim to have proven that the atomic structure of these alloys really is random. Firstly, this would require the exclusion of all conceivable models involving some short-range ordering, and secondly, we have not yet undertaken a systematic study in combination with the other experimental methods. This will be necessary in order to complete the informa-

tion about the atomic structure of the materials as we have outlined above. However, we could definitely show the experimental data to be compatible with the assumption of a random atomic arrangement.

A clear picture of the directional distribution of ionic coordinations can be derived only from the distribution of *both* splitting parameters  $V_{zz}$  and  $\eta$ . This in turn can be determined only for nuclei with spin  $I > \frac{3}{2}$ . Therefore, the nuclei most frequently employed in investigations of amorphous materials by Mössbauer spectroscopy,  $^{57}\text{Fe}$  and  $^{119}\text{Sn}$ , are not suited for this kind of study as in both cases the nuclear transition occurs between levels with spins  $\frac{1}{2}$  and  $\frac{3}{2}$ . Some good candidates would be  $^{73}\text{Ge}$ ,  $^{99}\text{Ru}$ ,  $^{121}\text{Sb}$ ,  $^{129}\text{I}$ ,  $^{157}\text{Gd}$ , and  $^{237}\text{Np}$ .

The results obtained from our investigation do have implications for problem areas beyond our specific subject, the relation between atomic structure of amorphous materials and the EFG distribution.

(i) The distribution of second-order crystal-field splittings is described by the same functions as that of nuclear quadrupole splittings. Our results apply directly to this problem which is important for the magnetic properties of amorphous rare-earth alloys.

(ii) The distribution function of magnetic dipolar fields in amorphous magnets<sup>46</sup> is closely related to the EFG distribution since the dipole field due to an ion carrying a magnetic moment is the product of the source moment with a tensor which has the same dependence upon the spatial coordinates of the source ion as the EFG tensor.

(iii) For the EFG distribution experienced instantaneously by nuclei in liquid metals the approximation derived for random ionic arrangements is applicable. In liquids of course, the EFG is rapidly changing with time, giving rise to nuclear quadrupole relaxation. In theoretical estimates of the fluctuation rate, mostly based on the fundamental work by Sholl<sup>47</sup> it has been assumed that the time-average of the EFG is zero. Sholl has argued that "... the average field gradient ... is zero since the average charge distribution about a given nucleus has spherical symmetry."<sup>47</sup> Although there is no doubt concerning the second part of Sholl's statement, his argument is not necessarily correct: The EFG is a functional of the charge density, and Sholl's argument would hold only if this operation and that of forming the average were interchangeable. This is not true in general. Since the time average and the configurational average of  $V_{zz}$  should have the same value, we conclude from the nonzero values of  $\langle V_{zz} \rangle_{\text{config}}$  obtained in our study that  $\langle V_{zz} \rangle_{\text{time}}$  in liquids may have a finite, nonzero value. In

monoatomic liquids, this average value presumably is very small, but in liquid alloys of elements whose ions carry different charges, a measurable average EFG may result.

#### ACKNOWLEDGMENTS

Discussions with R. W. Cochrane, R. Harris, and D. Quitmann about several aspects of our problem were very helpful. In the course of this work, we have profited repeatedly from critical comments and stimulating advice by P. Fulde.

#### APPENDIX: THE EFG DISTRIBUTION CAUSED BY TWO OR THREE IONS IN A SPHERICAL SHELL

For a small number  $N_I$  of ions in a spherical coordination shell, the distribution function  $F(D, S)$  for a given distribution of bond angles  $\Theta_{ij}$  can be derived on the basis of Eqs. (12) and (13) (Sec. II C). If all ions carry the same charge,  $q_i = q$ , and if all radial distances have the same value,  $r_i = r_s$ , Eqs. (12) and (13) can be simplified:

$$S = \left(\frac{q}{r_s^3}\right)^2 \left(3 \sum_{i < j} \cos^2 \Theta_{ij} - \frac{1}{2} N_I (N_I - 3)\right), \quad (\text{A1})$$

$$D = \left(\frac{q}{r_s^3}\right)^3 \left(27 \sum_{i < j < k} \cos \Theta_{ij} \cos \Theta_{ik} \cos \Theta_{jk} + 9(3 - N_I) \sum_{i < j} \cos^2 \Theta_{ij} + \frac{1}{2} N_I (3 - N_I) (3 - 2N_I)\right). \quad (\text{A2})$$

In the following we assume  $r_s$  to have some constant value.

For  $N_I = 2$ , the problem of finding the distribution function  $P_2(V_{zz}, \eta)$  is trivial. There is only one free parameter, the bond angle  $\Theta_{12}$ . We introduce the abbreviation  $y = \cos \Theta_{12}$  and express  $V_{zz}$  in terms of the contribution of a single ion,  $V_1 = q/r_s^3$ ,  $v = V_{zz}/V_1$ . If the ions have zero radius,  $r_I = 0$ , and for a random charge distribution,  $y$  is distributed uniformly in the range  $-1 \leq y \leq 1$ . Both  $v$  and  $\eta$  are functions of  $y$ :

$$\begin{aligned} v &= \frac{1}{2}(1 + 3y), \quad \eta = 3(1 - y)/(1 + 3y) \quad \text{for } \frac{1}{3} \leq y \leq 1 \\ v &= -1, \quad \eta = 3|y| \quad \text{for } -\frac{1}{3} \leq y \leq \frac{1}{3} \\ v &= \frac{1}{2}(1 - 3y), \quad \eta = 3(1 + y)/(1 - 3y) \quad \text{for } -1 \leq y < -\frac{1}{3}. \end{aligned} \quad (\text{A3})$$

For hard-sphere ions of finite radius  $r_I$ , the range of  $y$  is reduced to  $-1 \leq y \leq y_{\text{lim}} = 1 - 2(r_I/r_s)^2$ . The resulting marginal distributions  $Q(v)$  and  $R(\eta)$  for  $r_I = 0$ ,  $0.25r_s$ , and  $0.5r_s$  are shown in Fig. 8.

For a shell containing three ions the arrangement of the charges is described by three vari-

ables (apart from the irrelevant orientation of the entire shell given by the Euler angles  $\alpha, \beta, \gamma$ ), the three bond angles  $\Theta_{12}$ ,  $\Theta_{13}$ , and  $\Theta_{23}$ . We use again an abbreviated notation:  $y_1 = \cos \Theta_{12}$ ,  $y_2 = \cos \Theta_{13}$ ,  $y_3 = \cos \Theta_{23}$ . However, for given  $y_1$  and  $y_2$ , the third variable  $y_3$  is not completely free since the relation

$$y_3 = y_1 y_2 + (1 - y_1^2)^{1/2} (1 - y_2^2)^{1/2} \cos \phi \quad (\text{A4})$$

must be fulfilled. Here,  $\phi$  is the azimuthal angle at the apex defined by the ion with label "1" in the spherical triangle formed by the three ions. This angle can be considered as the third independent variable along with  $y_1$  and  $y_2$ . A random charge distribution is defined as a uniform distribution in this three-dimensional parameter space:

$$\Phi(y_1, y_2, \phi) dy_1 dy_2 d\phi = \frac{1}{8\pi} dy_1 dy_2 d\phi. \quad (\text{A5})$$

With help of Eq. (A4) this can be converted to an expression in terms of  $y_1, y_2, y_3$ :

$$\begin{aligned} \Phi(y_1, y_2, y_3) dy_1 dy_2 dy_3 \\ = \frac{1}{8\pi} (1 - y_1^2 - y_2^2 - y_3^2 + 2y_1 y_2 y_3)^{-1/2} dy_1 dy_2 dy_3. \end{aligned} \quad (\text{A6})$$

As for  $V_{zz}$ , we define reduced variables for  $S$  and  $D$ :

$$s = \frac{1}{3} S / V_1^2 = y_1^2 + y_2^2 + y_3^2, \quad d = \frac{1}{27} D / V_1^3 = y_1 y_2 y_3. \quad (\text{A7})$$

For the derivation of the distribution function  $F(d, s)$  from Eq. (A6) a third variable  $t$  is required such that a one-to-one correspondence exists between all points  $(y_1, y_2, y_3)$  and  $(d, s, t)$ . We define  $t = y_1 + y_2 + y_3$ . Then this correspondence is equivalent to the relation between the coefficients and the roots of the polynomial

$$\begin{aligned} p(y) &= (y - y_1)(y - y_2)(y - y_3) \\ &= y^3 - ty^2 + \frac{1}{2}(t^2 - s)y - d. \end{aligned} \quad (\text{A8})$$

This relation can be used to derive by some algebraic manipulations the distribution function:

$$F(d, s) ds dd = C(1 - s + 2d)^{-1/2} I(d, s), \quad (\text{A9})$$

where  $C$  is a normalization factor and  $I(d, s)$  is a sum of two integrals:

$$I(d, s) = \sum_{j=1}^2 \int_{t_1^{(j)}}^{t_2^{(j)}} dt [R(d, s, t)]^{-1/2} \quad (\text{A10})$$

with

$$\begin{aligned} R(d, s, t) &= 2s^3 - 108d^2 - 36sdt \\ &\quad - 5s^2t^2 + 20dt^3 + 4st^4 - t^6. \end{aligned} \quad (\text{A11})$$

This polynomial is the discriminant of  $p(y)$ . The



limits of integration  $t_i^{(j)}$  are defined by  $R(d, s, t_i^{(j)}) = 0$  and  $R(d, s, t) > 0$  in the range  $t_1^{(j)} < t < t_2^{(j)}$ .

Using Eq. (10) of Sec. II C, the function  $P_3(V_{zz}, \eta)$  is easily obtained from Eq. (A9). Figure 9(a) shows the resulting marginal distribution functions  $Q(V_{zz})$ ,  $R(\eta)$  [ $P(V_{zz}, \eta)$  integrated over all  $V_{zz}$ ],  $R_+(\eta)$  ( $V_{zz} > 0$ ), and  $R_-(\eta)$  ( $V_{zz} < 0$ ) and the comparison with the corresponding distributions obtained from computer experiments for ions with radius  $r_I = 0$ .

In the framework of a hard-sphere model, excluded volumes can be accounted for exactly. The formal expressions (A9)–(A11) remain unchanged, but the limits of the  $t$  integration are modified by the requirement that all  $y_i$  must have values less than the limiting value  $y_{\text{lim}} = 1 - 2(r_I/r_a)^2$ . Substituting  $y_{\text{lim}}$  into the polynomial  $p(y)$ , Eq. (A8), we obtain the excluded-volume limits for  $t$  for given values of  $s$ ,  $d$ , and  $y_{\text{lim}}$ :

$$t_{\text{lim}}^{(\pm)} = y_{\text{lim}} \pm (2d/y_{\text{lim}} + s - y_{\text{lim}}^2)^{1/2}. \quad (\text{A12})$$

Inspection of the derivative  $dy/dt$  for  $y = y_{\text{lim}}$  and  $t = t_{\text{lim}}$  shows that the range  $t_{\text{lim}}^{(-)} < t < t_{\text{lim}}^{(+)}$  has to be omitted from the integrals in Eq. (A10). The resulting marginal distribution functions in comparison with the distributions obtained from computer experiments for the case  $r_s = 2r_I$  are displayed in Fig. 9(b).

We have carried through the calculations for the case of a random distribution of the ionic charges. Any other structural model is treated by choosing the appropriate distribution function  $\Phi(y_1, y_2, y_3)$  of the bond angles in Eq. (A5). Because of the equivalence of the variables  $y_1, y_2, y_3$ , the function  $\Phi$  must be symmetric in these variables for any physically meaningful model. Thus, it can be expressed as a function  $\Psi(d, s, t)$ . The final result is again given by Eq. (A9) with Eq. (A10) replaced by

$$I(d, s) = \sum_{j=1}^2 \int_{t_1^{(j)}}^{t_2^{(j)}} dt \Psi(d, s, t) [R(d, s, t)]^{-1/2}. \quad (\text{A13})$$

\*Present address: Physical Laboratory, Trinity College, Dublin 2, Ireland.

†Laboratory associated with Université Scientifique et Médicale de Grenoble.

<sup>1</sup>G. S. Cargill III, in *Solid State Physics*, edited by H. Ehrenreich, F. Seitz, and D. Turnbull (Academic, New York, 1975), Vol. 30, p. 227.

<sup>2</sup>H. S. Chen and B. K. Park, *Acta Met.* **21**, 395 (1973).

<sup>3</sup>M. H. Cohen and F. Reif, in *Solid State Physics*, edited by F. Seitz and D. Turnbull (Academic, New York, 1957), Vol. 5, p. 321.

<sup>4</sup>B. D. Dunlop, in *Mössbauer Effect Data Index 1970*, edited by J. G. Stevens and V. E. Stevens (Plenum, New York, 1972), p. 25.

<sup>5</sup>R. M. Steffen and H. Frauenfelder, in *Perturbed Angular Correlations*, edited by E. Karlsson, E. Matthias, and K. Siegbahn (North-Holland, Amsterdam, 1964), p. 1.

<sup>6</sup>A review on investigations by Mössbauer spectroscopy containing many references to relevant original publications was given by J. M. D. Coey, *J. Phys. (Paris) Colloq.* **35**, C6-89 (1974). For a similar review on NMR studies see P. C. Taylor, E. J. Friebele, and M. Rubinstein, in *Physics of Structurally Disordered Solids*, edited by S. S. Mitra (Plenum, New York, 1976), p. 665.

<sup>7</sup>D. Sarkar, R. Segnan, E. K. Cornell, E. Callen, R. Harris, M. Plischke, and M. J. Zuckermann, *Phys. Rev. Lett.* **32**, 542 (1974); R. W. Cochrane, R. Harris, M. Plischke, D. Zobin, and M. J. Zuckermann, *Phys. Rev. B* **5**, 1969 (1975).

<sup>8</sup>M. E. Lines, *Phys. Rev. B* **20**, 3729 (1979); M. Eibschütz, M. E. Lines, and K. Nassau, *ibid.* **21**, 3767 (1980).

<sup>9</sup>P. Heubes, D. Korn, G. Schatz, and G. Zibold, *Phys. Lett.* **74A**, 267 (1979).

<sup>10</sup>J. Szeftel and H. Alloul, *Phys. Rev. Lett.* **42**, 1691 (1979).

<sup>11</sup>D. C. Price, S. J. Campbell, and P. J. Back, *J. Phys. (Paris) Colloq.* **41**, C1-263 (1980).

<sup>12</sup>M. Henry, F. Varret, J. Teillet, G. Ferey, O. Massenet, and J. M. D. Coey, *J. Phys. (Paris) Colloq.* **41**, C1-279 (1980).

<sup>13</sup>R. W. Cochrane, R. Harris, M. Plischke, D. Zobin, and M. J. Zuckermann, *J. Phys. F* **5**, 763 (1975).

<sup>14</sup>M. I. Darby and G. R. Evans, *Phys. Status Solidi B* **85**, K63 (1978).

<sup>15</sup>R. Harris, M. Plischke, and M. J. Zuckermann, *Phys. Rev. Lett.* **31**, 160 (1973); R. W. Cochrane, R. Harris, and M. J. Zuckermann, *Phys. Rep.* **48**, 2 (1978).

<sup>16</sup>One has to be cautious when applying the assumption of isotropy to real materials. The unidirectional character of the most frequently employed methods of preparation such as evaporation, sputtering, and sputter cooling, may induce some anisotropy in the final product.

<sup>17</sup>J. M. Ziman, *Models of Disorder* (Cambridge University Press, Cambridge, 1979).

<sup>18</sup>E. N. Kaufmann and R. J. Vianden, *Rev. Mod. Phys.* **51**, 161 (1979).

<sup>19</sup>R. S. Raghavan, E. N. Kaufmann, and P. Raghavan, *Phys. Rev. Lett.* **34**, 1280 (1975).

<sup>20</sup>M. L. Mehta, *Random Matrices* (Academic, New York, 1967).

<sup>21</sup>A. Abragam, *Principles of Nuclear Magnetism* (Oxford University Press, Oxford, 1961).

<sup>22</sup>H. Goldstein, *Classical Mechanics* (Addison-Wesley, Reading, Mass., 1959), pp. 107–109.

<sup>23</sup>C. E. Porter and N. Rosenzweig, *Suomalaisen Tiedekatemian Toimituksia A VI*, No. 44 (1960). The formula and its derivation are also given in Ref. 20, pp. 30–33.

- <sup>24</sup>R. G. Palmer and C. M. Pond, *J. Phys. F* **9**, 1451 (1979).
- <sup>25</sup>A. Fert and I. A. Campbell, *J. Phys. F* **8**, L57 (1978). Unfortunately these authors have introduced an asymmetry parameter  $\eta_{Fc}$  which is different from the usual definition of  $\eta$ . The relation between  $\eta_{Fc}$  and  $\eta$  furthermore depends upon the sign of  $V_{zz}$ :  $\eta_{Fc} = \pm 3(\eta - 1)/(\eta + 3)$  for  $V_{zz} \gtrless 0$ .
- <sup>26</sup>P. Garoche, A. Fert, J. J. Veyssié, and B. Boucher, *J. Magn. Magn. Mater.* **15-18**, 1397 (1980). In this paper the same asymmetry parameter  $\eta_{Fc}$  as in Ref. 25 is used.
- <sup>27</sup>M. L. Mehta, *Random Matrices*, Ref. 20, p. 24. There proof is given that all invariants of a symmetrical  $N \times N$  matrix  $\bar{V}$  can be expressed in terms of the  $N$  quantities  $\text{trace}(\bar{V}^n)$ ,  $n = 1, 2, \dots, N$ . The equivalence of the determinant of  $\bar{V}$  and of  $\text{trace}(\bar{V}^N)$  is easily shown.
- <sup>28</sup>K. Adkins and N. Rivier, *J. Phys. (Paris) Colloq.* **35**, C4-237 (1974).
- <sup>29</sup>The definition of the density parameter  $\rho$  in Eq. (14) corresponds to the relative packing density of hard spheres in a plane, that is, to the limit  $(r_s/r_l) \rightarrow \infty$ . For finite  $r_s$  an exact general definition can not be given as truly dense packing is only possible for certain discrete values of the ratio  $(r_s/r_l)$ . The numerical factors relating the maximum number of ions in a shell, corresponding to  $\rho = 1$ , to  $(r_s/r_l)^2$  vary from case to case. For the first coordination shell with  $r_s/r_l = 2$ , the value of this factor is 3. This is not very far from the value given in Eq. (14), which we have chosen since the considerations in this section concern the region of large values for the ratio  $r_s/r_l$ . Other choices for the factor do not materially affect our arguments and the results.
- <sup>30</sup>W. Feller, *An Introduction to Probability Theory and its Applications* (Wiley, New York, 1966), Vol. 2, pp. 252-259.
- <sup>31</sup>The basic random variables are the angular coordinates of the individual ions. Thus, for large  $N_l$  there are many degrees of freedom ( $2N_l - 3$ ), and the distribution of one of the parameters  $U_m$  is not substantially affected by the small number of restrictions imposed by choosing definite values for the other variables  $U_{m'}$  with  $m' \neq m$ . The argument is essentially the same as that employed in establishing the equivalence of the different ensembles (grand canonical, canonical, and microcanonical) in statistical thermodynamics.
- <sup>32</sup>The marginal distribution functions  $R_+(\eta)$  and  $R_-(\eta)$  are defined by integration of  $P(V_{zz}, \eta)$  only over positive or negative values of  $V_{zz}$ , respectively.
- <sup>33</sup>J. D. Bernal, *Proc. R. Soc. London, Ser. A* **280**, 299 (1964).
- <sup>34</sup>A. Pustówka, B. D. Sawicka, and J. A. Sawicki, *Phys. Status Solidi B* **57**, 783 (1973).
- <sup>35</sup>P. J. Unsworth, *Proc. Phys. Soc. London, Sect. A* **2**, 122 (1969).
- <sup>36</sup>F. J. van Steenwijk, H. T. Lefever, R. C. Thiel, and K. H. J. Buschow, *Physica (Utrecht)* **92B**, 52 (1977).
- <sup>37</sup>J. M. D. Coey, J. Chappert, J.-P. Rebouillat, and T. S. Wang, *Phys. Rev. Lett.* **36**, 1061 (1976).
- <sup>38</sup>K. Ruebenbauer, J. Fink, H. Schmidt, G. Czjzek, and K. Tomala, *Phys. Status Solidi B* **84**, 611 (1977).
- <sup>39</sup>K. Tomala, G. Czjzek, J. Fink, and H. Schmidt, *Solid State Commun.* **24**, 857 (1977).
- <sup>40</sup>A. Amamou [*Solid State Commun.* **33**, 1029 (1980)] reported significant shifts of the 3d bands in amorphous Zr-Co and Zr-Ni alloys. Similar but weaker shifts have been observed in amorphous Gd 3d alloys (P. Oelhafen, private communication).
- <sup>41</sup>J.-P. Rebouillat, A. Liénard, J. M. D. Coey, R. Arrese-Boggiano, and J. Chappert, *Physica (Utrecht)* **86-88B**, 773 (1977).
- <sup>42</sup>A. J. Freeman, in *Magnetic Properties of Rare Earth Metals*, edited by R. J. Elliott (Plenum, New York, 1972), p. 323.
- <sup>43</sup>M. T. Hutchings, in *Solid State Physics*, edited by F. Seitz and D. Turnbull (Academic, New York, 1964), Vol. 16, p. 227.
- <sup>44</sup>B. D. Dunlap, G. K. Shenoy, and G. M. Kalvius, *Phys. Rev. B* **10**, 26 (1974); their result has been questioned recently by S. Ahmad and D. J. Newman, *J. Phys. C* **12**, 1245 (1979).
- <sup>45</sup>An alternative method is the determination of the distribution of crystal-field splittings by inelastic neutron scattering. Application of this method will be restricted to rare-earth ions as only these have a sufficiently large scattering cross section. Experiments of this type with liquid rare earths have been reported by A. H. Millhouse and A. Furrer, *Phys. Rev. Lett.* **35**, 1231 (1975).
- <sup>46</sup>M. Fähnle, *J. Magn. Magn. Mater.* **15-18**, 133 (1980).
- <sup>47</sup>C. A. Sholl, *Proc. Phys. Soc. London* **91**, 130 (1967).